

Technique for bulk Fermiology by photoemission applied to layered ruthenates

A. Sekiyama,¹ S. Kasai,¹ M. Tsunekawa,¹ Y. Ishida,¹ M. Sing,^{1,2} A. Irizawa,¹ A. Yamasaki,¹ S. Imada,¹ T. Muro,³ Y. Saitoh,^{3,4} Y. Onuki,⁵ T. Kimura,^{6,*} Y. Tokura,⁶ and S. Suga¹

¹*Department of Material Physics, Graduate School of Engineering Science, Osaka University, Toyonaka, Osaka 560-8531, Japan*

²*Experimentalphysik II, Universität Augsburg, D-86135 Augsburg, Germany*

³*Japan Synchrotron Radiation Research Institute, SPring-8, Mikazuki, Hyogo 679-5198, Japan*

⁴*Department of Synchrotron Research, Kansai Research Establishment, Japan Atomic Energy Research Institute, SPring-8, Mikazuki, Hyogo 679-5148, Japan*

⁵*Department of Physics, Graduate School of Science, Osaka University, Toyonaka, Osaka 560-0043, Japan*

⁶*Department of Applied Physics, University of Tokyo, Tokyo 113-8656, Japan*

(Dated: November 19, 2018)

We report the Fermi surfaces of the superconductor Sr_2RuO_4 and the non-superconductor $\text{Sr}_{1.8}\text{Ca}_{0.2}\text{RuO}_4$ probed by bulk-sensitive high-energy angle-resolved photoemission. It is found that there is one square-shaped hole-like, one square-shaped electron-like and one circle-shaped electron-like Fermi surface in both compounds. These results provide direct evidence for nesting instability giving rise to magnetic fluctuations. Our study clarifies that the electron correlation effects are changed with composition depending on the individual band.

PACS numbers: 79.60.-i, 71.18.+y, 74.70.Pq

Clarification of Fermi surfaces (FSs) is fundamental to understand the physical properties of functional materials such as superconducting transition metal oxides, heavy fermion systems, and organic conductors. Quantum oscillation measurements by virtue of the de Haas-van Alphen or Shubnikov-de Haas effect are known as useful techniques to detect bulk FSs. However, their electron- or hole-like character and their shape cannot be experimentally revealed by these measurements alone. In addition, these techniques require low temperatures and almost defect-free single crystals, so that they are not easily applicable to doped or partially substituted systems such as the high-temperature superconductors $\text{La}_{2-x}\text{Sr}_x\text{CuO}_4$, $\text{Bi}_2\text{Sr}_2\text{CaCu}_2\text{O}_{8+\delta}$, or the here reported $\text{Sr}_{1.8}\text{Ca}_{0.2}\text{RuO}_4$. The number of measurements by using quantum oscillations on oxides is actually very few. On the other hand, low-energy angle-resolved photoemission (ARPES) is known as a tool for probing FSs as well as quasi-particle dispersions of correlated electron systems.¹ However, it is still unclear whether so far reported low-energy ARPES ($h\nu \lesssim 120$ eV) results fully reflect bulk electronic structures because of its high surface-sensitivity. Since high-energy photoemission ($h\nu \geq 500$ eV) has an advantage in probing bulk states,^{2,3} high-energy ARPES with high angular resolution can be a complementary and promising technique for the bulk Fermiology of solids besides the quantum oscillations measurements.

It is known that Sr_2RuO_4 shows "triplet" superconductivity^{4,5}, which disappears with a very small amount of Ca-substitution.⁶ Combination of the quantum oscillation measurements and band-structure calculations suggests one hole-like FS sheet centered at (π, π) (α sheet) and two electron-like FS sheets centered at $(0,0)$ (β and γ sheets) in Sr_2RuO_4 .^{7,8,9} On the other hand, so far re-

ported results of low-energy ARPES for Sr_2RuO_4 are controversial although ARPES has an advantage in determining the character of FSs. Yokoya *et al.* have first concluded two hole-like and one electron-like FSs.¹⁰ However, the following ARPES studies^{1,11,12} have suggested that the earlier finding originates from surface states, and that the bulk FSs are qualitatively similar to the result of the band-structure calculation. It has also been reported that a lattice distortion takes place at the surface,¹³ giving FSs different from the bulk. Thus the characters and shapes of the two-dimensional bulk FSs of Sr_2RuO_4 are experimentally still unclear because the reported shapes of the FSs from the low-energy ARPES depend on the surface preparation and the excitation photon energies.^{11,12} Low-energy ARPES on Sr_2RuO_4 has shown that the FSs shapes measured on the "degraded" surface obtained by cleavage at 180 K and fast cooled down seem to be similar to the prediction of the band-structure calculation compared with those on the clean surface prepared by cleavage at 10 K.^{1,12} In general, photoemission data on cleaner surfaces prepared by cleavage at lower temperatures, at which surface desorption and diffusion of atoms from inside are suppressed, are more reliable. Thus the mere similarity of the FSs as obtained by low-energy ARPES and theory cannot guarantee that the genuine bulk FSs of Sr_2RuO_4 are really established. Besides, the FSs of lightly Ca-substituted $\text{Sr}_{1.8}\text{Ca}_{0.2}\text{RuO}_4$ are not yet clarified at all.

Compared with low-energy ARPES, high-energy ARPES faces several experimental difficulties regarding the detection of quasi-particle dispersions and FSs. High angular resolution is especially required for high-energy ARPES since the momentum resolution not only depends on the angular resolution but also on the square root of the photoelectron kinetic energy ($\sim h\nu$ in the

case of the valence-band ARPES). Furthermore, a high photon flux is also required for a practical high-energy ARPES measurement because photoionization cross sections decrease exponentially with $h\nu$.¹⁴ Recent improvements in both synchrotron light sources and electron spectrometers allow us to measure high-energy ARPES spectra with high angular and energy resolutions facilitating bulk Fermiology. In this paper, we show the FSSs of $\text{Sr}_{2-x}\text{Ca}_x\text{RuO}_4$ probed for the first time by means of high-energy ARPES.

Single crystals of $\text{Sr}_{2-x}\text{Ca}_x\text{RuO}_4$ ($x = 0, 0.2$) were used for the measurements. The high-energy ARPES measurements at $h\nu = 700$ eV were performed at BL25SU in SPring-8.¹⁵ The base pressure was about 4×10^{-8} Pa. The (001) clean surface was obtained by cleaving the samples *in situ* at the measuring temperature of 20 K. The photoelectrons within polar angles of about $\pm 6^\circ$ with respect to the normal of the sample surface were simultaneously collected by using a GAMMADATA-SCIENITA SES200 analyzer, thereby covering more than a whole Brillouin zone along the direction of the analyzer slit. The overall energy resolution was set to ~ 120 and ~ 200 meV for high-resolution measurements and Fermi surface-mapping, respectively. The angular resolution was $\pm 0.1^\circ$ ($\pm 0.15^\circ$) for the perpendicular (parallel) direction to the analyzer slit, which was experimentally confirmed at BL25SU. These values correspond to the momentum resolution of $\pm 0.024 \text{ \AA}^{-1}$ ($\pm 0.035 \text{ \AA}^{-1}$) [6 and 9 % of π/a , where a is the lattice constant of Sr_2RuO_4 , 3.87 \AA (Ref. 4)] at $h\nu = 700$ eV. The surface cleanliness was confirmed by means of the angle-integrated photoemission by the absence of additional spectral weight on the higher binding energy side of the intrinsic O 1s contribution, absence of the possible C 1s signal, and no peak or hump structure at 9 – 10 eV from E_F in the spectra. We also measured core-level spectra with an energy resolution of 200 meV.

Figure 1 shows the polar-angle (θ) dependence of the Sr 3d core-level spectra of Sr_2RuO_4 . The surface contributions in the spectra is enhanced with increasing θ . In addition to peaks at 132 and 134 eV originating from the 3d spin-orbit splitting, two shoulder structures appear on the higher binding energy side of the main peaks in the spectrum at $\theta = 0^\circ$. The intensity of these shoulders is remarkably enhanced in the more surface-sensitive spectrum at $\theta = 60^\circ$. Therefore the main peaks and the additional structures are ascribed to the bulk and surface components, respectively. A more detailed analysis shows that there is actually another surface component in the spectra.¹⁶ Due to this analysis, both spectra are well deconvoluted into the bulk and two surface contributions (S1 and S2) with the intensity ratio of Bulk : S1 : S2 = 0.58 : 0.26 : 0.16 at $\theta = 0^\circ$ and 0.36 : 0.39 : 0.25 at $\theta = 60^\circ$. These ratios are very close to what we expect from the lattice constants and the calculated photoelectron mean free path¹⁷ at the kinetic energy of 565 eV ($\lambda = 12.3 \text{ \AA}$), namely, 0.59 : 0.24 : 0.17 at $\theta = 0^\circ$ and 0.35 : 0.43 : 0.22 at $\theta = 60^\circ$. Since λ at the photoelec-

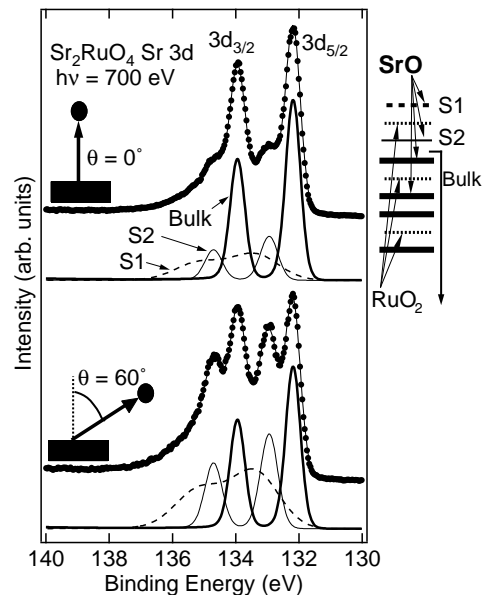


FIG. 1: Polar-angle (θ) dependence of the Sr 3d core-level photoemission spectra of Sr_2RuO_4 (filled circles). The spectra are well deconvoluted into three components corresponding to the contributions from the top-most SrO surface layer (S1), the second SrO surface layer (S2) placed just below the top RuO_2 layer, and the bulk layers.

tron kinetic energy of 700 eV is calculated as 13.5 \AA, the bulk contribution in the valence-band spectra at $\theta \sim 0^\circ$ is estimated as 63 %. It was demonstrated in V_2O_3 that the surface component is noticeably suppressed near the Fermi level (E_F) due to its more localized character.¹⁸ Namely, the stronger electron correlation in the surface than in the bulk leads to less quasi-particle weight near E_F and enhanced spectral weight of the surface component away from E_F in the spectra of various transition metal oxides. Likewise the surface spectral weight is expected at higher binding energies away from E_F than the bulk spectral weight near E_F in $\text{Sr}_{2-x}\text{Ca}_x\text{RuO}_4$.

Let us show the ARPES spectra [energy distribution curves (EDCs)] of Sr_2RuO_4 along the $(\pi, 0)$ - (π, π) direction in Fig. 2(a), which demonstrate that a band starts from ~ 0.5 eV at $(\pi, 0)$, approaches to and crosses the Fermi level (E_F) on going to the (π, π) direction. The peak width becomes narrower near E_F . This quasi-particle forms the hole-like FS sheet α . A similar behavior is observed in $\text{Sr}_{1.8}\text{Ca}_{0.2}\text{RuO}_4$ as shown in Fig. 2(b). However, the peak is broader in the spectra for $x = 0.2$ near the Fermi wave vector (k_F) compared with those for $x = 0$.

The ARPES spectra of $\text{Sr}_{2-x}\text{Ca}_x\text{RuO}_4$ along the $(0, 0)$ - $(\pi, 0)$ cut are shown in Figs. 2(c) and 2(d). They are rather complicated because there are three quasi-particle bands below E_F in this direction. For both compounds, the band forming the α sheet is located at ~ 0.5 eV, which shifts hardly between $(0, 0)$ and $(\pi, 0)$, while the other two bands forming the β and γ sheets show dispersion and

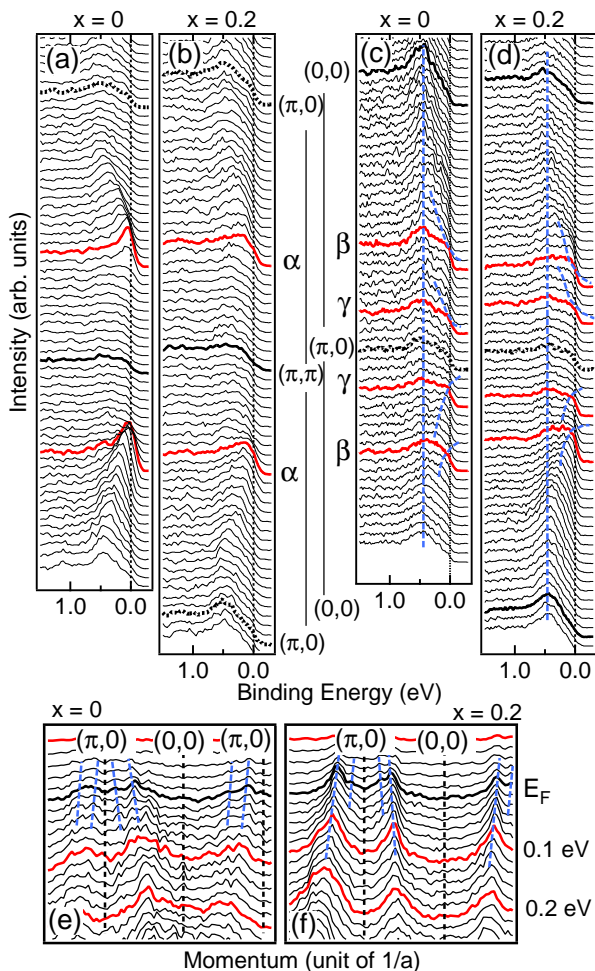


FIG. 2: High-energy ARPES spectra near E_F of $\text{Sr}_{2-x}\text{Ca}_x\text{RuO}_4$. (a) EDCs along the $(\pi,0)$ - (π,π) cut of Sr_2RuO_4 with an energy resolution of ~ 200 meV. The red lines show the spectra where the quasi-particle band crosses E_F (i.e., at k_F). (b) Same as (a) for $\text{Sr}_{1.8}\text{Ca}_{0.2}\text{RuO}_4$. (c) EDCs along the $(0,0)$ - $(\pi,0)$ direction of Sr_2RuO_4 with an energy resolution of ~ 120 meV. The blue dashed lines indicate the band dispersions. (d) Same as (c) for $\text{Sr}_{1.8}\text{Ca}_{0.2}\text{RuO}_4$. (e) MDCs along the $(0,0)$ - $(\pi,0)$ cut of Sr_2RuO_4 . (f) Same as (e) for $\text{Sr}_{1.8}\text{Ca}_{0.2}\text{RuO}_4$.

cross E_F . The behavior of the E_F crossing of the β and γ branches (hereafter abbreviated as β and γ crossing) is also confirmed by the momentum distribution curves (MDCs) as shown in Figs. 2(e) and 2(f), and the symmetrized EDCs with respect to E_F (not shown in this paper, a similar procedure was used in Ref. 11). The behavior of the ARPES spectra for $\text{Sr}_{1.8}\text{Ca}_{0.2}\text{RuO}_4$ is qualitatively similar to that of Sr_2RuO_4 whereas subtle differences can be recognized as the quasi-particle of the β sheet is more prominent for $\text{Sr}_{1.8}\text{Ca}_{0.2}\text{RuO}_4$ than for Sr_2RuO_4 whereas the E_F crossing of the γ sheet is less prominent than for $x = 0$.

The photoemission intensity at E_F for $\text{Sr}_{2-x}\text{Ca}_x\text{RuO}_4$ and estimated Fermi wave vectors¹⁹ k_F 's are displayed in

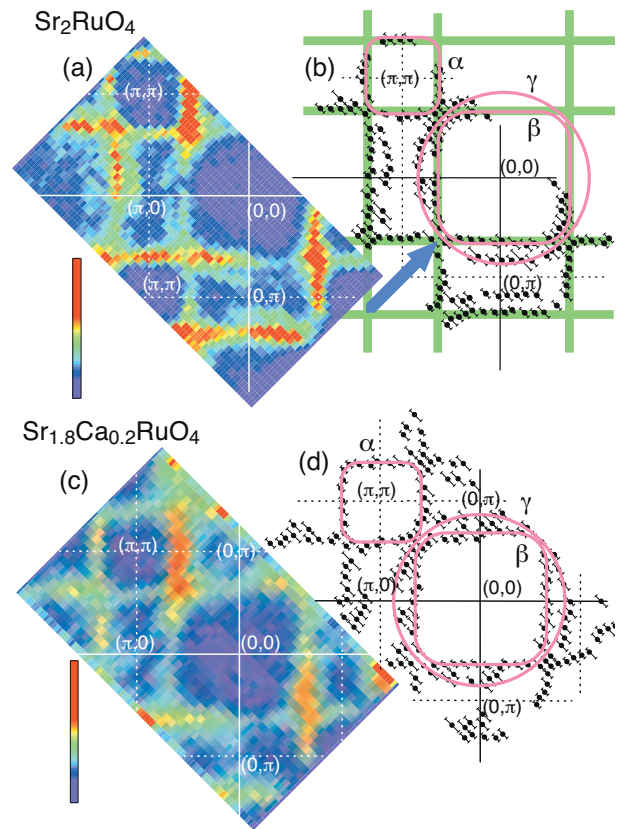


FIG. 3: Fermi surfaces of $\text{Sr}_{2-x}\text{Ca}_x\text{RuO}_4$ obtained from the high-energy ARPES. (a) Photoemission intensity map integrated from E_F to -0.1 eV (unoccupied energy side), which represents the FSs of Sr_2RuO_4 . (b) Estimated k_F and schematically drawn FSs (pink solid curves) based on our results. The bold green lines show two one-dimensional FSs mutually orthogonalized, as a result of the combination of the obtained two square-like FSs, α and β sheets. The blue arrow represents the feasible nesting vector. (c) Same as (a) for $\text{Sr}_{1.8}\text{Ca}_{0.2}\text{RuO}_4$. (d) Same as (b) for $\text{Sr}_{1.8}\text{Ca}_{0.2}\text{RuO}_4$.

Fig. 3. One can clearly identify the one hole-like (α) and the two electron-like (β and γ) FS sheets. We find that the shapes of the α and β sheets are square-like while the shape of the γ sheet is rather circular-like for both compounds. These shapes reflect that the γ sheet is mainly composed of a rather ideally two-dimensional d_{xy} band while the other square-shaped sheets are due to the d_{yz} and d_{zx} bands, which are to some extent one-dimensional in the electronic states. The estimated area of each sheet is comparable to the results from the quantum oscillations for Sr_2RuO_4 . The obtained FSs of $\text{Sr}_{1.8}\text{Ca}_{0.2}\text{RuO}_4$ are similar to those of Sr_2RuO_4 . The two-dimensional topology of the FSs is also consistent with the prediction from band-structure calculations.^{8,9}

The combination of the observed two square-like FS sheets, the α and β sheets, can also be regarded as two

one-dimensional FSs located at $k_x = \pm Q$ and $k_y = \pm Q$, where Q is estimated as $\sim 0.65\pi$ from our high-energy ARPES. It has been theoretically predicted that FS nesting effect occurs with wave vectors $\mathbf{q} = (\pm 2\pi/3, k'_y)$, $\mathbf{q} = (k'_x, \pm 2\pi/3)$ and especially at $\mathbf{q} = (\pm 2\pi/3, \pm 2\pi/3)$ where k'_y and k'_x are arbitrary.²⁰ An inelastic neutron scattering study indeed detected magnetic fluctuations for $\mathbf{q}_0 = (\pm 0.6\pi, \pm 0.6\pi)$, which could be due to the nesting properties.²¹ As shown in Fig. 3, the observed FSs give direct evidence for the nesting instability with $\mathbf{q} = (\pm 2\pi/3, \pm 2\pi/3)$.

For $\text{Sr}_{1.8}\text{Ca}_{0.2}\text{RuO}_4$, the γ crossing cannot be resolved in some k -regions whereas the β crossing is clearly detected almost everywhere in reciprocal space [Figs. 3(c) and 3(d)]. This is somewhat different from our FS map of Sr_2RuO_4 , where also the γ -crossing can be resolved almost everywhere [Figs. 3(a) and 3(b)] and the spectral weight at k_F is comparable between the β and γ sheets in most of the k -regions. As for the α sheet, a reduced quasi-particle weight at E_F is observed for $x = 0.2$ compared with that for $x = 0$ as shown in Fig. 2. From these facts we conclude that the electron correlations become stronger for the α and γ sheets by the small amount of Ca-substitution ($x < 0.5$), which does not lead any lattice distortion.²²

Although the electron correlation strengths seem to be changed depending on the individual band between the superconducting Sr_2RuO_4 and the non-superconducting

$\text{Sr}_{1.8}\text{Ca}_{0.2}\text{RuO}_4$, the electronic structures are found to be qualitatively unchanged. On the other hand, it has been reported that the superconductivity in Sr_2RuO_4 is easily suppressed by impurities and/or defects.^{23,24} From these facts, we can conclude that the superconductivity disappears with the Ca-substitution because the substituted Ca ions behave as "impurity" and/or induce disorder in $\text{Sr}_{2-x}\text{Ca}_x\text{RuO}_4$, and therefore break the superconductivity, as proposed by Nakatsuji and Maeno.⁶

To conclude, the bulk-sensitive high-energy ARPES study of $\text{Sr}_{2-x}\text{Ca}_x\text{RuO}_4$ has revealed the character and the shape of FS sheets, and the nesting instability. We are convinced that high-energy ARPES measurements are crucial for really revealing the bulk FSs of many transition metal oxides.

We thank T. Satonaka, H. Fujiwara, A. Higashiya, P. T. Ernst, A. Shigemoto, and T. Sasabayashi for supporting the experiments. This work was supported by a Grant-in-Aid for COE Research (10CE2004) and Creative Scientific Research (15GS0213) from the Ministry of Education, Culture, Sports, Science and Technology (MEXT), Japan. M.S. is grateful for financial support by the Japan Society for the Promotion of Science (JSPS). The ARPES measurements were performed under the approval of the Japan Synchrotron Radiation Research Institute (2001A0128-NS-np, 2002B3009-LS-np, and 2003A4009-LS-np).

* Present Address: Los Alamos National Laboratory, Los Alamos, NM 87545

- ¹ A. Damascelli, Z. Hussain, and Z.-X. Shen, *Rev. Mod. Phys.* **75**, 473 (2003).
- ² A. Sekiyama, T. Iwasaki, K. Matsuda, Y. Saitoh, Y. Ōnuki, and S. Suga, *Nature* **403**, 396 (2000).
- ³ A. Sekiyama, K. Kadono, K. Matsuda, T. Iwasaki, S. Ueda, S. Imada, S. Suga, R. Settai, H. Azuma, Y. Ōnuki, and Y. Saitoh, *J. Phys. Soc. Jpn.* **69**, 2771 (2000).
- ⁴ Y. Maeno, H. Hashimoto, K. Yoshida, S. Nishizaki, T. Fujita, J. G. Bednorz, and F. Lichtenberg, *Nature* **372**, 532 (1994).
- ⁵ K. Ishida, H. Mukuda, Y. Kitaoka, K. Asayama, Z. Q. Mao, Y. Mori, and Y. Maeno, *Nature* **396**, 658 (1998).
- ⁶ S. Nakatsuji and Y. Maeno, *Phys. Rev. Lett.* **84**, 2666 (2000).
- ⁷ T. Oguchi, *Phys. Rev. B* **51**, 1385 (1995).
- ⁸ A. P. Mackenzie, S. R. Julian, A. J. Diver, G. J. McMullan, M. P. Ray, G. G. Lonzarich, Y. Maeno, S. Nishizaki, and T. Fujita, *Phys. Rev. Lett.* **76**, 3786 (1996).
- ⁹ Y. Yoshida, R. Settai, Y. Ōnuki, H. Takei, K. Betsuyaku, and H. Harima, *J. Phys. Soc. Jpn.* **67**, 1677 (1998).
- ¹⁰ T. Yokoya, A. Chainani, T. Takahashi, H. Katayama-Yoshida, M. Kasai, and Y. Tokura, *Phys. Rev. Lett.* **76**, 3009 (1996).
- ¹¹ A. V. Puchkov, Z.-X. Shen, T. Kimura, and Y. Tokura, *Phys. Rev. B* **58**, R13322 (1998).
- ¹² A. Damascelli, D. H. Lu, K. M. Shen, N. P. Armitage, F. Ronning, D. L. Feng, C. Kim, Z.-X. Shen, T. Kimura, Y.

Tokura, Z. Q. Mao, and Y. Maeno, *Phys. Rev. Lett.* **85**, 5194 (2000).

- ¹³ R. Matzdorf, Z. Fang, Ismail, J. Zhang, T. Kimura, Y. Tokura, K. Terakura, and E. W. Plummer, *Science* **289**, 746 (2000).
- ¹⁴ J. J. Yeh and I. Lindau, *At. Data Nucl. Data Tables* **32**, 1 (1985).
- ¹⁵ Y. Saitoh, H. Kimura, Y. Suzuki, T. Nakatani, T. Matsushita, T. Muro, T. Miyahara, M. Fujisawa, K. Soda, S. Ueda, H. Harada, M. Kotsugi, A. Sekiyama, and S. Suga, *Rev. Sci. Instrum.* **71**, 3254 (2000).
- ¹⁶ For the analysis of core-level spectra, a symmetric line shape (Lorentzian with Gaussian broadening) is used for each component. The Lorentzian width is assumed to be independent of components (~ 0.06 eV) while the Gaussian width is changed depending on components. Origins of the different Gaussian widths among components are not clear at present. Asymmetry of the core-level line shapes originates generally from excited electron-hole pairs in the vicinity of E_F due to the core-level excitation on the same sites. Since there is no Sr-derived conduction electron near E_F , the line shapes of the Sr $3d$ core level should be almost symmetric. The Shirley-type background is also added in the fitted spectra.
- ¹⁷ S. Tanuma, C. J. Powell, and D. R. Penn, *Surf. Sci.* **192**, L849 (1987).
- ¹⁸ S.-K. Mo, J. D. Denlinger, H.-D. Kim, J.-H. Park, J. W. Allen, A. Sekiyama, A. Yamasaki, K. Kadono, S. Suga, Y. Saitoh, T. Muro, P. Metcalf, G. Keller, K. Held, V. Ey-

- ert, V. I. Anisimov, and D. Vollhardt, Phys. Rev. Lett. **90**, 186403 (2003).
- ¹⁹ We have determined k_F 's by the criteria listed below, which are commonly used in ARPES studies: (1) peak dispersion extrapolated to E_F , (2) intensity maxima in the MDCs at and slightly above (≤ 0.1 eV) E_F , (3) momentum where the peak closest to E_F drastically changes its intensity and disappears.
- ²⁰ I. I. Mazin and D. J. Singh, Phys. Rev. Lett. **82**, 4324 (1999).
- ²¹ Y. Sidis, M. Braden, P. Bourges, B. Hennion, S. Nishizaki, Y. Maeno, and Y. Mori, Phys. Rev. Lett. **83**, 3320 (1999).
- ²² O. Friedt, M. Braden, G. André, P. Adelman, S. Nakatsuji, and Y. Maeno, Phys. Rev. B **63**, 174432 (2001).
- ²³ A. P. Mackenzie, R. K. W. Haselwimmer, A. W. Tyler, G. G. Lonzarich, Y. Mori, S. Nishizaki, and Y. Maeno, Phys. Rev. Lett. **80**, 161 (1998).
- ²⁴ S. Nishizaki, Y. Maeno, S. Farner, S. Ikeda, and T. Fujita, J. Phys. Soc. Jpn. **67**, 560 (1998).

* Present Address: Los Alamos National Laboratory, Los Alamos, NM 87545